J Mater Sci (2017) 52:663–673

Synergistic catalytic effect of light rare earth element and other additives on the degree of graphitization and properties of graphite

Rongyan Wang[1], Guimin Lu[1,*], Haizheng Zhuang[1], and Jianguo Yu[1,2]

[1] *National Engineering Research Center for Integrated Utilization of Salt Lake Resources, Shanghai 200237, People's Republic of China*

[2] *State Key Laboratory of Chemical Engineering, East China University of Science and Technology, Shanghai 200237, People's Republic of China*

Received: 14 July 2016
Accepted: 31 August 2016
Published online: 14 October 2016

ABSTRACT

Metal additives usually have a catalytic effect on non-graphitic carbon materials. However, graphitic carbon materials are difficult to catalyze owing to carbon atoms whose neighbors are ordered regions and less cross-linked. Artificial graphite is generally prepared from coke and pitch, both of which are graphitic carbon. Therefore, efficient catalysts for graphitic carbon materials are important for industrial technology. The effect of light rare earth elements (La, Ce, and Pr) and other additives (Ti, Ni, and B) as co-catalysts in artificial graphite development was investigated. Compared with the single catalysts, the combinatorial catalysts more significantly improved the degree of graphitization in the carbon materials, indicating synergistic catalytic effects. Both dissolution–precipitation and formation–decomposition of carbide were involved in the synergistic catalytic mechanisms. In the combinatorial catalysts systems, the light rare earth element would accelerate the graphitization process of carbon materials by widening the range of the catalytic temperature, accelerating the speed of oversaturation of dissolution, or generating a new carbide phase with the other catalyst. This would promote formation of the more-ordered graphitic structure at relatively low temperature. For instance, to attain the same degree of graphitization and better crystalline sizes at the same residence time, the carbon materials with combinatorial catalysts can be heat treated at temperatures 400 °C lower than without catalysts, and the electrical and mechanical properties are enhanced.

Address correspondence to E-mail: gmlu@ecust.edu.cn

DOI 10.1007/s10853-016-0359-9

Introduction

As a semiconductor with a distinctive crystal structure, graphite has a wide range of useful properties, making it an interesting material in technology [1–3]. The degree of graphitization plays an important role in the thermal conductivity, electrical conductivity, and mechanical properties. Catalytic graphitization with numerous catalysts has been proposed to accelerate the graphitization process and improve the degree of graphitization at relatively low temperature [3–14].

Recently, alloys or compounds have been investigated as catalysts owing to their synergistic catalytic effect on the degree of graphitization of carbon materials [15–26]. The majority of studies have focused on the synergistic catalytic effect of catalysts containing one metallic additive and one inorganic additive, although some studies have investigated catalysts with two metallic additives. Tzeng et al. reported that the degree of graphitization is enhanced in electroless Ni–P-coated polyacrylonitrile-based carbon fibers heat treated at 1400 °C compared with uncoated fibers heat treated at 2400 °C [15, 16]. Garcia et al. found that Ni–Si has a synergistic catalytic effect on the structural properties of carbon nanofibers produced by catalytic decomposition of methane [17]. Moreover, the microstructures of carbon fibers were improved after being coated with Ti–B, or Ni–B, or doped with Mo–B [18–20]. Carbon materials doped with Ti–Si have also attracted attention because of the notable enhancement of the ordered graphitic structure [3, 21]. Synergistic catalysis corresponded to the combination type of catalysts which contain one metallic additive and one inorganic additive mentioned above. It was considered that formation–decomposition of carbide occurred in these carbon materials along with formation of a new phase by reaction of the metallic catalyst with another additive. However, the mechanism of the combination type of catalysts which contain two metallic additives follows the rule that both dissolution–precipitation and formation–decomposition of carbide simultaneously occur. Significant effects have been attained in carbon materials using catalysts of Fe–Ni, Fe–Co, and Ti–Ni alloys/compounds [7, 22–26].

In our previous research, we found that a small amount of a light rare earth (RE) element significantly improves the properties of carbon material [27, 28]. For instance, 1 wt% praseodymium oxide significantly catalyzes graphitization of the graphite anode. However, there are few reports of synergistic catalytic graphitization of carbon materials using light RE elements and other additives. In this study, in combination with light RE element (La, Ce or Pr) additives, Ti and Ni were selected to represent two categories whose mechanisms have been proposed to follow different routes [3, 29]. Boron was also considered as an additive with light RE element because of its special homogeneous effect on catalytic graphitization of carbon materials [30]. The influence of the heat-treatment temperature and the effect of combinatorial catalysts on the microstructure and mechanical properties of graphite were investigated.

Materials and methods

Preparation

Coal-based needle coke and coal tar pitch were used as an aggregate and a binder, respectively. The additives were added to the mixture (coke:pitch = 4:1, wt/wt). The typical procedure to produce artificial graphite was then carried out, including kneading, hot molding, baking and impregnation, and finally graphitization. The sources and properties of the raw materials and the detailed experimental procedures are described elsewhere [28]. The samples are labeled as G–$X_1Y_1X_2Y_2$/Z, where G is graphite, X_1 and X_2 are the additives, Y_1 and Y_2 are the amounts of the additives (wt%), and Z is the temperature at which the sample was treated.

Characterization

The effect of combinatorial catalysts on the microstructures of graphite was investigated by X-ray diffraction (XRD, Riguku D/max-2550 diffractometer with Cu Kα1 radiation, $\lambda = 1.5406$ Å). The interlayer spacing (d_{002}), degree of graphitization (g), and mean crystalline size along c-axis (L_c) of the samples were examined with silicon as the internal standard, and then calculated using the appropriate equations (Bragg, Mering-Maire and Alexander equations) [31, 32].

Raman measurements of surface sections of the samples were performed with a Thermo DXR spectrograph at an excitation wavelength of 445 nm.

Ten Raman spectra were collected for each sample because the lattice vibration is strongly influence by charged impurities [33, 34]. The D, G, and 2D peaks were fitted with Lorentz functions. The degree of graphitization was determined by the intensity ratio of the D to G peaks (I_D/I_G). The mean crystalline size along the *a*-axis (L_a) was calculated using the Cançado equation [35].

The morphologies of the samples were observed by transmission electron microscopy (TEM, JEOL/JEM 2100).

The electrical resistivity of graphite at room temperature was measured by the DC four-probe method.

Three-point bending flexural tests were performed on a universal testing machine (3300 Instron) for samples with dimensions of 10 × 10 × 40 mm and a span-length of 30 mm. For each system, three samples were tested at a loading speed of 2 mm min^{-1} to obtain an average value. The bending strength was calculated by (1):

$$\sigma = 1.5PL\left(BH^2\right)^{-1}, \quad (1)$$

where P is the maximum flexural load, L is the span-length, and B and H are the width and the height of samples, respectively.

Results

The crystal parameters of the graphitized samples calculated from the XRD patterns and Raman spectra are listed in Table 1, including the d_{002}, g, I_D/I_G, L_a, and L_c values.

Compared with the G/2800 sample, all of the graphite samples prepared with the Ti additive have

Table 1 Crystal parameters of the graphitized samples determined from the XRD patterns and Raman spectra

Sample	d_{002} (nm)	g (%)	I_D/I_G	L_a (nm)	L_c (nm)
G/2800	0.3366	86.05	0.202	46.6	66.2
G–Ti0.5/2800	0.3363	89.53	0.096	98.2	67.2
G–Ti1.0/2800	0.3362	91.02	0.119	79.0	74.1
G–Ti2.0/2800	0.3362	90.70	0.093	101	84.9
G–Ti3.0/2800	0.3361	91.86	0.089	106	89.0
G–Ti4.0/2800	0.3360	91.14	0.097	98.4	94.9
G–Ti5.0/2800	0.3360	93.02	0.092	103	96.4
G–Ti3.0La1.0/2800	0.3359	94.44	0.101	93.2	98.3
G–Ti3.0Ce1.0/2800	0.3361	91.98	0.097	97.4	97.1
G–Ti3.0Pr1.0/2800	0.3358	95.30	0.109	86.7	98.4
G–Ti4.0/2400	0.3370	81.09	0.299	31.5	78.4
G–Ti3.0La1.0/2400	0.3369	82.69	0.285	33.0	88.1
G–Ti3.0Ce1.0/2400	0.3367	84.87	0.264	35.6	84.5
G–Ti3.0Pr1.0/2400	0.3366	85.74	0.272	34.6	89.0
G–Ni4.0/2800	0.3357	96.75	0.140	67.4	118
G–Ni3.0La1.0/2800	0.3360	93.28	0.105	90.0	83.2
G–Ni3.0Ce1.0/2800	0.3356	97.76	0.112	84.3	89.0
G–Ni3.0Pr1.0/2800	0.3359	93.71	0.159	59.3	86.5
G–Ni4.0/2400	0.3370	81.82	0.187	43.7	81.0
G–Ni3.0La1.0/2400	0.3367	84.44	0.188	50.2	83.0
G–Ni3.0Ce1.0/2400	0.3367	84.73	0.178	52.8	82.9
G–Ni3.0Pr1.0/2400	0.3369	82.11	0.215	50.4	85.1
G–B4.0/2800	0.3357	96.17	0.203	46.3	96.9
G–B3.0La1.0/2800	0.3359	94.00	0.234	40.3	93.9
G–B3.0Ce1.0/2800	0.3358	95.44	0.216	43.5	93.0
G–B3.0Pr1.0/2800	0.3359	93.71	0.125	75.6	90.2
G–B4.0/2400	0.3367	84.87	0.243	38.7	80.4
G–B3.0La1.0/2400	0.3368	84.15	0.242	38.8	82.8
G–B3.0Ce1.0/2400	0.3363	89.52	0.333	28.2	86.4
G–B3.0Pr1.0/2400	0.3366	86.33	0.212	44.4	81.7

lower d_{002} values, larger crystalline sizes (both L_a and L_c), and higher degrees of graphitization. The L_c value shows a similar trend to the d_{002} value. Compared with the G–Ti4.0/2800 sample, the samples with the same combinatorial catalyst content (3 wt% Ti and 1 wt% light RE element) have lower d_{002} values and higher degrees of graphitization. The g values are higher at the higher heat-treatment temperature in all the cases. The effect of the heat-treatment temperature on the L_c value is similar to that on the g value, while the effect on the L_a value is more prominent. The effect of the heat-treatment temperature on the L_a value in samples prepared with the Ti additive is the most significant, followed by that in the samples prepared with Ni and B additives. For the heat-treatment temperature of 2400 °C, all of the samples prepared with combinatorial catalysts have lower d_{002} values, higher degrees of graphitization, and larger L_c values than the corresponding samples prepared with a single additive. However, the L_a values are similar for samples prepared with a single catalyst and the combinatorial catalysts.

Compared with the G/2800 sample, the as-prepared samples with Ti and RE catalysts have similar d_{002} values but larger L_c values when they were heat treated at 2400 °C. Similar results are observed in the cases of G–Ni3.0RE1.0/2400 and G–B3.0RE1.0/2400. Moreover, the L_a values of the samples with Ni and RE catalysts heat treated at 2400 °C are larger than that of the samples without catalyst heat treated at 2800 °C. However, the L_a values of the G–Ti3.0RE1.0/2400 and G–B3.0RE1.0/2400 samples are all lower than that of the G/2800 sample.

A TEM image showing the lamellae morphology of the G–Ti4.0/2800 sample is shown in Fig. 1. All of the layers are parallel to the lamellar plane, which is clearly shown in the enlarged image of the area indicated by the white rectangle. Highly ordered stacked layers with a d_{002} value of 0.3360 nm are observed, indicating that a high degree of graphitization was achieved.

To investigate the synergistic catalytic effect of the combination catalysts, wide-angle XRD patterns were firstly recorded to confirm the structure and phases of the graphitized samples, as shown in Fig. 2. The sharp peaks of hexagonal graphite are easily observed. With increasing heat-treatment temperature, the (100) peak becomes sharper and more symmetrical, as expected. Along with the peaks of graphite, diffraction peaks of TiC and RE carbide

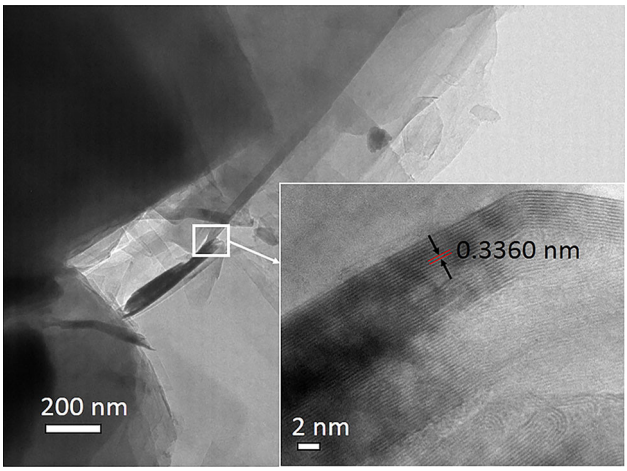

Figure 1 HRTEM image of the graphitized sample with 4.0 wt% Ti after heat treatment at 2800 °C. The *inset* shows the d_{002} interlayer spacing of 0.3360 nm.

(REC_2) are observed in Fig. 2a. For the G–Ni–RE samples (Fig. 2b), signals corresponding to the nickel RE carbide ($RENiC_2$) phase are detected in the samples heat treated at 2400 °C. In the G–B–RE samples heat treated at 2400 °C (Fig. 2c), the peak at around 32° is attributed to REC_2. However, REC_2 is not detected for the heat-treatment temperature of 2800 °C, as shown in Fig. 2f.

Figure 3 shows the representative Raman spectra. When the heat-treatment temperature was increased from 2400 to 2800 °C, the D and G peaks in the Raman spectrum of the G–Ti4.0 sample became sharper and the I_D/I_G ratio increased, indicating that the degree of graphitization increased. This tendency is also observed for the G–Ni4.0 and G–B4.0 samples. The positions of the peaks in samples prepared with the co-catalysts are similar to the corresponding samples prepared with the single catalysts.

The as-prepared samples heat treated at 2800 °C were processed by the machining method to obtain specimens suitable for measuring the electrical resistivity and mechanical properties. The bulk density and electrical resistivity of the as-prepared samples are listed in Table 2. All of the graphitized samples prepared with catalysts show lower electrical resistivity than the sample prepared without a catalyst.

The effects of Ti and RE elements doped at the same amount on the mechanical properties of the samples were compared, as shown in Fig. 4a. Figure 4b shows a comparison of the effect of different catalysts on the bending stress of the samples.

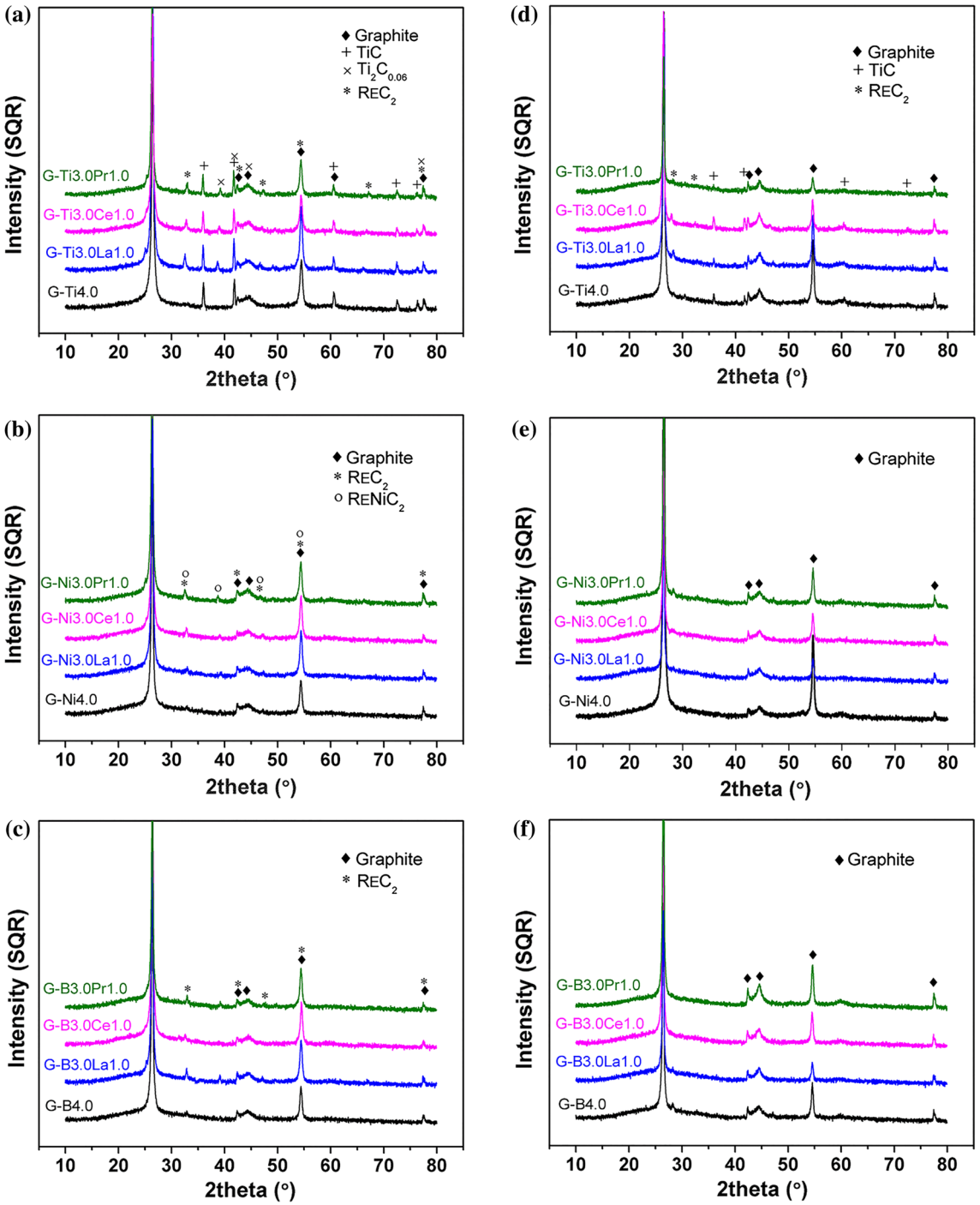

Figure 2 XRD patterns of graphite prepared with additives at **a**–**c** 2400 °C and **d**–**f** 2800 °C.

Discussion

Determination of the amount of catalysts added into the carbon materials

As the results show, Ti enhances the crystallinity of carbon materials at 2800 °C, which is consistent with other publications [18, 21]. However, the catalytic effect of Ti did not increase with increasing Ti content, which is supported by the weakly fluctuant values of g, I_D/I_G, and L_a. This is consistent with the results reported by He et al., who proposed that formation of titanium carbide (TiC) is the reason for a similar phenomenon in carbon fibers doped with Ti [18]. Consequently, 3 wt% Ti was added to

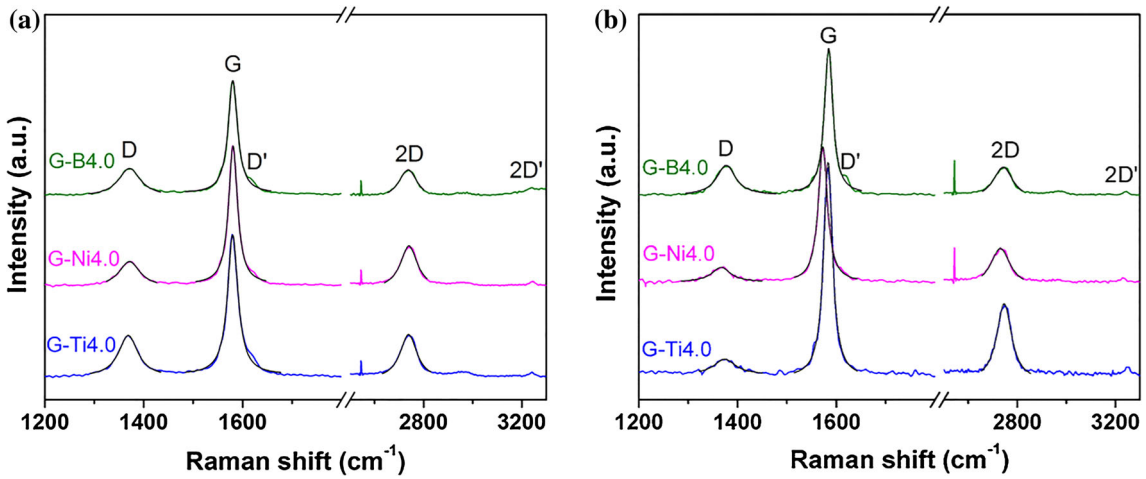

Figure 3 Raman spectra of graphite prepared with single catalysts at **a** 2400 °C and **b** 2800 °C.

Table 2 Bulk densities and electrical resistivity of graphite samples prepared with and without catalysts at 2800 °C

Samples	Bulk density (g cm^{-3})	ρ (μΩ m)
G/2800	1.61	8.5
G–Ti4.0/2800	1.71	6.4
G–Ti3.0La1.0/2800	1.71	5.9
G–Ti3.0Ce1.0/2800	1.70	6.5
G–Ti3.0Pr1.0/2800	1.71	5.4
G–Ni4.0/2800	1.64	7.7
G–Ni3.0La1.0/2800	1.66	7.8
G–Ni3.0Ce1.0/2800	1.62	6.4
G–Ni3.0Pr1.0/2800	1.65	7.3
G–B4.0/2800	1.64	7.4
G–B3.0La1.0/2800	1.70	6.5
G–B3.0Ce1.0/2800	1.72	6.1
G–B3.0Pr1.0/2800	1.71	6.8

the as-prepared samples with 1 wt% of a light RE element as a second additive to investigate their synergistic catalytic effect on graphite. The reason for choosing 1 wt% of the light RE element was based on the finding that 1 wt% of praseodymium oxide significantly influenced the graphitization process and then improved the electrical properties of the graphite anode in our previous publication [28]. In addition, other catalysts (Ni and B) with the same content were also prepared with the same process to compare the synergistic catalytic effects.

Graphitized samples with additives heat treated at different temperatures

The highest degree of graphitization (with a d_{002} value of 0.3358 nm) was achieved in the sample with 3 wt% Ti–1 wt% Pr. This indicates that the combination of Ti and a light RE element has an effect on the microstructure of graphite.

However, this phenomenon was not observed for the G–Ni–RE and G–B–RE samples. A single Ni or B additive had a more significant effect on d_{002} than the corresponding combinatorial catalysts, which can be attributed to the L_c value, as mentioned above. The reason for this is related to their different catalytic mechanisms, which will be discussed latter.

Generally, the effect of temperature on the graphitization of carbon materials is significant, and catalysts are used to accelerate the graphitization process at relatively low temperature [1, 3]. The degree of structural order of samples increased as the heat-treatment temperature of the precursor increases, finally leading to graphitic materials. In previous publications [15–20], the carbon fibers, whose raw materials were hard carbon, such as methane, furan resin, and polyacrylonitrile, were catalyzed by the combinatorial catalysts which contain one metallic additive and one inorganic additive at about 2400–2800 °C for 2 h. Since hard carbon was easier to accept the assistance of catalysts than soft carbon [36], the graphite, whose raw materials were coke and mesophase pitch, doped with Ti and Si were heat treated at 2400–2600 °C and under 8–10 MPa hot-pressing simultaneously [21]. In this study, the carbon precursor were needle coke and coal tar pitch, which were both the soft carbon raw materials, and the graphite was obtained from these carbon precursor by adding light rare earth elements and other typical catalysts and heat treated at 2800 °C for 0.5 h.

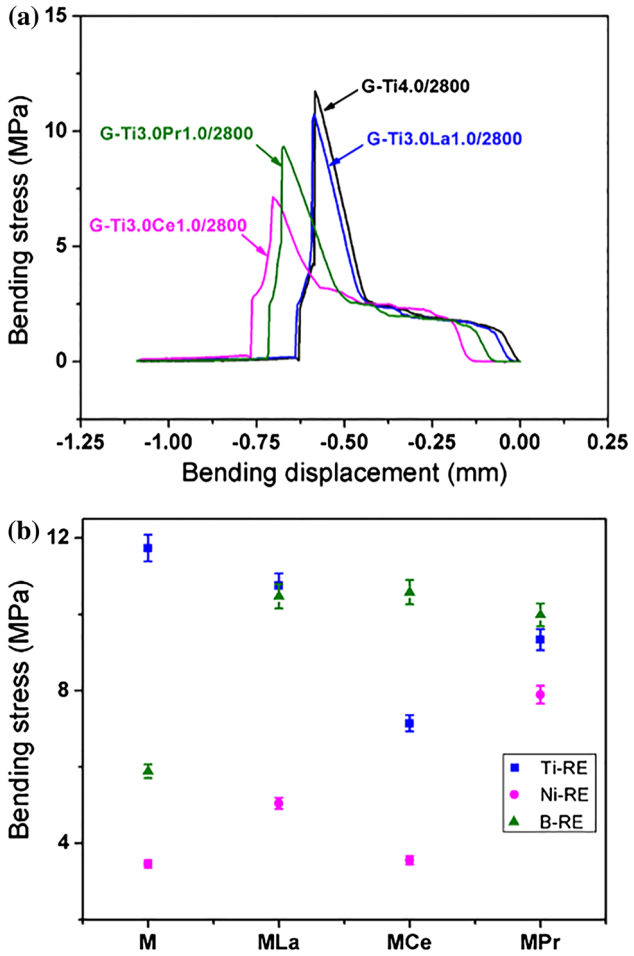

Figure 4 **a** Representative bending stress–displacement curves of G–Ti–RE samples heat treated at 2800 °C. **b** Comparison of the effect of different additives on the bending stress of the samples. M represents the metal.

This indicated that the light rare earth elements exhibited the more significant catalytic ability than other catalysts and may assist the other catalysts to catalyze the soft carbon materials.

The difference between the L_a value and other crystalline parameters can be explained as follows: the L_a value calculated by Raman spectroscopy is affected by the technique based on propagation of phonons. This propagation is only stopped by the boundaries of the layers (or by a "physical end" or by defects bordering the layers) [1]. Vacancy defects formed after the departure of boron can be detected, and the L_a values are smaller for B than the other additives at both temperatures.

Comparison of the heat-treatment results in Table 1 leads to the conclusion that for a given temperature, more-ordered structures are obtained for samples prepared with combinatorial catalysts than a single catalyst, which indicates a synergistic catalytic effect on the graphitization of carbon materials. For instance, the G–Ti4.0/2400, G–Ti3.0Pr1.0/2400, G–B4.0/2400, and G–B3.0Pr1.0/2400 samples have L_c values of ~78, ~89, ~80, and ~86 nm, respectively. The sample prepared with a B–Ce co-catalyst has a d_{002} value of 0.3363 nm and an L_c value of 86.4 nm after heat treatment at 2400 °C, suggesting a synergistic catalytic effect. For the samples prepared with Ti catalysts, the d_{002} values are lower than that of the G–Ti4.0 sample at both temperatures, and the L_c values are higher in the G–Ti–RE samples. However, this trend is only observed for the Ni and B catalysts at a heat-treatment temperature of 2400 °C.

According to the values of the crystal parameters, the catalysts played an important role during the graphitization of carbon materials at relatively low temperature. The combinational catalysts synergistically accelerate the graphitization process, and thus the more-ordered graphitic structure can be obtained at lower temperature.

Synergistic catalytic effect during the graphitization process

For the Ti catalysts, as well as the peaks from the graphite phases, there are extra peaks corresponding to TiC shown in Fig. 2, which is consistent with the previous studies [2, 9]. The chemical stability of TiC means that it is difficult to decompose. Therefore, a decrease in the intensity of the TiC phase with increasing temperature indicates enhancement of graphitization.

Because REC_2 peaks are present in the XRD patterns of the samples heat treated at 2400 °C, formation of graphite at the expense of carbide decomposition seems to be a plausible mechanism for catalytic graphitization of these carbon materials. The intensities of the REC_2 peaks decrease when the heat-treatment temperature of the samples increases, and the peaks are not present in the XRD patterns of the samples prepared at 2800 °C. However, it cannot be concluded that REC_2 decomposes to the metal and graphite with increasing temperature. Compared with G/2800, the residual TiC and REC_2 at 2400 °C results in an increase of grain boundaries and defects, and subsequently leads to a decrease of the L_a value calculated from the Raman spectra.

Nickel carbide was not detected, although it probably formed. It decomposes at temperatures above 500 °C [24, 29]. Ni accelerates graphitization followed a dissolution–precipitation mechanism, which means the disordered carbon dissolves into the liquid Ni phase and subsequently precipitated as graphite [6, 12, 19]. Similar to REC_2, $RENiC_2$ peaks are not present in the XRD patterns of the samples prepared at 2800 °C. Combined with the results for the G–Ti–RE samples, these results demonstrate that the catalytic behavior of the metals in the combinatorial catalysts involves formation of carbide by the reaction of the metal catalyst with carbon and its subsequent decomposition to graphite. This explains why the L_a values of the G–Ni–RE samples heat treated at 2400 °C are larger than that of the G/2800 sample (i.e., because of evaporation of Ni and little residual carbide).

No boron or boron carbide phases were detected, which is similar to nickel carbide. In previous publications, boron was considered to accelerate graphitization by creating local strain, which is the driving force when boron attacks and replaces specific free carbon atoms [30, 38]. Boron was not observed to react with the RE elements to form a new phase. Boron would result in defects, irrespective of its departure or substitution, leading to a decrease of the L_a value.

The results indicate that in the G–Ti–RE system, TiC and REC_2 are the primary catalysts that accelerate the graphitization process of carbon materials with high-temperature heat treatment. TiC is difficult to decompose once it is generated, while REC_2 exhibits different physical properties where formation and decomposition as well as melting occur. In the G–Ni–RE and G–B–RE systems, departure of Ni and B from graphite can entrain REC_2 to some degree, resulting in a decrease in the intensity of REC_2 at relatively high temperatures. REC_2 accelerates the graphitization process by not only its decomposition but also assisting dissolution–precipitation by accelerating the speed of oversaturation.

Although the XRD data are consistent with the Raman results, the carbides are not detected in the Raman spectrum [39]. All of the positions of the peaks correspond to graphite, including the sharp G peak and the weak D peak. The spectrum also shows a second-order peak of the D band at $\sim$2700 cm^{-1}, which is sometimes called the 2D or G′ band because it appears in more graphitic carbons materials. Dresselhaus et al. [40] suggested that the G′ band is a Raman-allowed mode for sp^2 carbons. Based on the concept of propagation of phonons in the Raman spectrum, the effect of carbides may be contained in the D and G bands owing to obstruction of the catalysts, which increase the edges of the layers or acts as heteroatom to connect continuous layers even if they are more or less wrinkled [37].

In the samples prepared with RE catalysts, the parameters calculated from the Raman spectra can be referenced to changes in the intensity (Table 1). Compared with G/2800, the G–Ni–RE samples have more graphitic order when they are heat treated at 2400 °C, which can also be detected by Raman spectroscopy. However, similar results were not obtained for the G–Ti–RE and G–B–RE systems. Based on the above experimental observations and analysis, light RE elements and other catalysts have a synergetic effect on graphitization of carbon materials. Synergistic catalytic mechanisms are proposed along with the corresponding binary phase diagrams.

It can be inferred that Ti and light RE element act as co-catalysts in the graphitization process of carbon materials based on coke and pitch by formation of TiC and REC_2, respectively. All of the decomposition temperatures of REC_2 are much lower than that of TiC ($\sim$2250 and 2776 °C, respectively), which means that light RE elements would accelerate the graphitization progress of carbon materials at relatively low temperature. In our previous publication [28], it was proposed that the light RE elements began to exhibit the catalytic effects when the carbon materials heat treated at 1600 °C. Therefore, the light RE elements and Ti catalyzed the carbon materials at different temperature ranges, respectively. Adding light RE elements widen the range of the catalytic temperature, improving the degree of graphitization. The catalytic mechanism was supported by the fact that all of the samples for G–Ti–RE systems have lower d_{002} values, higher degrees of graphitization, and larger L_c values than the corresponding samples prepared with a single additive both at different temperatures. The increase of the L_a values for G–Ti–RE systems after heat treated at 2400 °C confirmed that the light RE elements assisted the growth of the graphitic order structures at relatively low temperature.

The light RE elements in the G–Ni–RE systems had a similar effect on development of the graphitic structure at 2400 °C. For the Ni systems, $RENiC_2$ is in

the liquid state where carbon can dissolve to form an oversaturated solution. When the carbon materials heat treated above 1327 °C, the molten catalyst Ni was not only assist the diffusion of light RE elements but also reacted with part of light RE elements to create new phase $RENiC_2$. Then the decomposition of solid phase $RENiC_2$ occurred at higher heat-treatment temperature to release both light RE elements and graphite. This light RE elements can further catalyzed other less-ordered carbon. However, unlike $RENiC_2$, which further decomposed to graphite, the role of REC_2 in the Ni systems is similar to that in the Ti systems. However, the effect of it appears to be less significant than that in the Ti systems, as listed in Table 1. The main catalytic mechanism of Ni for carbon materials is preferential dissolution of disordered carbon and precipitation of graphite [18]. Hence, in all of the G–Ni–RE samples, the catalytic process follows the sequence of dissolution–precipitation and simultaneously carbide formation and decomposition.

However, light RE elements and B do not have a synergetic catalytic effect because no carbides were generated. Therefore, the microstructures of the G–B–RE samples are not attributed to the synergistic effect of the catalysts.

According to the above analysis, the active metals preferentially react with disordered carbons at the boundaries of the graphitic sheets to form the corresponding carbide, and further decomposition would lead to graphite. The presence of the metal catalysts increased the crystalline sizes of the already existing graphitic layers. When added to carbon materials with other catalysts, RE elements would assist catalytic graphitization.

Effect of combinatorial catalysts on the electrical and mechanical properties of graphitized samples

The electrical and mechanical properties of the graphitized samples were investigated based on the analysis of the crystal parameters and the catalytic process.

As summarized in our previous study [28], the L_c value is the most important factor for the electrical resistivity, followed by the bulk density and the degree of graphitization. The lowest electrical resistivity was obtained for the G–Ti3.0Pr1.0/2800 sample. Based on the microstructures and electrical properties of the samples, the light RE elements assist catalytic graphitization of samples with other additives, and the light RE elements and other catalysts have a synergistic effect.

Ti has a more significant enhancing effect on the mechanical properties than the RE elements. This was also found in Ref. [21], where the bending stress in graphite was significantly enhanced by doping with Ti. However, when Si was introduced as an additive in graphite doped with Ti, the value of the bending stress sharply decreased, demonstrating the different effects of the catalysts. RE elements showed the opposite effect in the G–Ni–RE and G–B–RE systems, especially in G–B–RE, as shown in Fig. 4(b).

The synergistic catalytic effect of Ti and RE elements was exhibited in the microstructures and electrical properties of graphite because of acceleration of catalytic graphitization within a wide temperature interval and the low electrical resistivity and high fracture strength of residual TiC and REC_2 [21]. The mechanical properties of graphite improved using Ni–RE catalysts because of the synergistic catalytic effect of Ni and the RE element. The departure of Ni would be harmful to graphite but this is compensated for by the RE element, which is also observed for the B–RE catalysts.

Conclusions

Three light RE elements (La, Ce, and Pr) were combined with other catalysts (Ti, Ni, and B) and added to carbon materials as co-catalysts to investigate their synergistic catalytic effect. The effect of the combinatorial catalysts on the degree of graphitization in the carbon materials was significant. Compared with reference samples containing the same amount of the single catalyst, more-ordered graphite was obtained using the combinatorial catalysts at a heat-treatment temperature of 2400 °C. Moreover, the as-prepared samples obtained with combinatorial catalysts had similar d_{002} values and larger L_c values when heat treated at 2400 °C compared with the sample without an additive heat treated at 2800 °C. This indicates that the RE elements and other catalysts have a synergistic catalytic effect on carbon materials. For instance, the combination of Ti and Pr had a synergistic catalytic effect on the microstructure of graphite, and the lowest electrical resistivity of 5.4 μΩ m was obtained after heat treatment at 2800 °C. In the

Ti–RE catalytic system, RE elements would accelerate graphitization of carbon materials by widening the range of the catalytic temperature. In the G–Ni–RE and G–B–RE systems, departure of the Ni and B can entrain REC_2, and the mechanisms include dissolution–precipitation and carbide formation and decomposition. The RE element compensates for the harm caused by departure of Ni. This was also was observed for the B–RE catalysts.

Acknowledgments

This work was supported by the National Science Foundation of China [Grant Number U1407202].

References

[1] Ōya A, Marsh H (1982) Review: Phenomena of catalytic graphitization. J Mater Sci 17:309–322

[2] Chung DDL (2002) Review: Graphite. J Mater Sci 37:1475–1489

[3] Lin Q, Feng Z, Liu Z, Guo Q, Hu Z, He L et al (2015) Atomic scale investigations of catalyst and catalytic graphitization in a silicon and titanium doped graphite. Carbon 88:252–261

[4] Maldonado-Hodar FJ, Moreno-Castilla C, Rivera-Utrilla J, Hanzawa Y, Yamada Y (2000) Catalytic graphitization of carbon aerogels by transition metals. Langmuir 16:4367–4373

[5] Liu T, Luo R, Yoon SH, Mochida I (2010) Anode performance of boron-doped graphites prepared from shot and sponge cokes. J Power Sources 195:1714–1719

[6] Liu YC, Liu QL, Gu JJ, Kang DM, Zhou FY, Zhang W et al (2013) Highly porous graphitic materials prepared by catalytic graphitization. Carbon 64:132–140

[7] Bacsa RR, Cameán I, Ramos A, Garcia AB, Tishkova V, Bacsa WS et al (2015) Few layer graphene synthesis on transition metal ferrite catalysts. Carbon 89:350–360

[8] Niu YA, Zhang X, Wu J, Zhao JP, Yan XQ, Li Y (2014) Catalytic and enhanced effects of silicon carbide nanoparticles on carbonization and graphitization of polyimide films. RSC Adv 4:42569–42576

[9] Kim J, Lee J, Choi Y, Jo C (2014) Synthesis of hierarchical linearly assembled graphitic carbon nanoparticles via catalytic graphitization in SBA-15. Carbon 75:95–103

[10] Tang J, Wang T, Sun X, Guo YX, Xue HR, Guo H et al (2013) Effect of transition metal on catalytic graphitization of ordered mesoporous carbon and Pt/metal oxide synergistic electrocatalytic performance. Micropor Mesopor Mat 177:105–112

[11] Lebedeva IV, Knizhnik AA, Popov AM, Potapkin BV (2012) Ni-assisted transformation of graphene flakes to fullerenes. J Phys Chem C 116:6572–6584

[12] Rodríguez-Manzo JA, Pham-Huu C, Banhart F (2011) Graphene growth by a metal-catalyzed solid-state transformation of amorphous carbon. ACS Nano 5:1529–1534

[13] Kumar R, Dhakate SR, Mathur RB (2013) The role of ferrocene on the enhancement of the mechanical and electrochemical properties of coal tar pitch-based carbon foams. J Mater Sci 48:7071–7080

[14] Aykut Y, Pourdeyhimi B, Khan SA (2013) Catalytic graphitization and formation of macroporous-activated carbon nanofibers from salt-induced and H_2S-treated polyacrylonitrile. J Mater Sci 48:7783–7790

[15] Tzeng SS (2006) Catalytic graphitization of electroless Ni–P coated PAN-based carbon fibers. Carbon 44:1986–1993

[16] Tzeng SS, Lin YH (2008) The role of electroless Ni–P coating in the catalytic graphitization of PAN-based carbon fibers. Carbon 46:555–558

[17] Garcia AB, Camean I, Pinilla JL, Suelves I, Lazaro MJ, Moliner R (2010) The graphitization of carbon nanofibers produced by catalytic decomposition of methane: synergetic effect of the inherent Ni and Si. Fuel 89:2160–2162

[18] He D, Zhang F, Xu S, Yu W, Cai Q, LaTempa TJ et al (2008) Synergistic catalytic effect of Ti–B on the graphitization of polyacrylonitrile-based carbon fibers. Carbon 46:1506–1508

[19] Zhou H, Yu Q, Peng Q, Wang H, Chen J, Kuang Y (2008) Catalytic graphitization of carbon fibers with electrodeposited Ni–B alloy coating. Mater Chem Phys 110:434–439

[20] Xu SH, Zhang FY, Liu SH, He DM, Cai QY (2010) Catalytic graphitization of Mo-B-doped polyacrylonitrile (PAN)-based carbon fibers. J Cent South Univ Technol 17:703–707

[21] Qiu H, Song Y, Liu L, Zhai G, Shi J (2003) Thermal conductivity and microstructure of Ti-doped graphite. Carbon 41:973–978

[22] Bokhonov B, Korchagin M (2002) The formation of graphite encapsulated metal nanoparticles during mechanical activation and annealing of soot with iron and nickel. J Alloy Compd 333:308–320

[23] Yang S, Chen X, Kikuchi N, Motojima S (2008) Catalytic effects of various metal carbides and Ti compounds for the growth of carbon nanocoils (CNCs). Mater Lett 62:1462–1465

[24] Xu SH, Zhang FY, Kang Q, Liu SH, Cai QY (2009) The effect of magnetic field on the catalytic graphitization of phenolic resin in the presence of Fe-Ni. Carbon 47:3233–3237

[25] Anton R (2009) In situ TEM investigations of reactions of Ni, Fe and Fe–Ni alloy particles and their oxides with amorphous carbon. Carbon 47:856–865

[26] Zhou HH, Peng QL, Huang ZH, Yu Q, Chen JH, Kuang YF (2011) Catalytic graphitization of PAN-based carbon fibers with electrodeposited Ni-Fe alloy. Trans Nonferrous Met Soc China 21:581–587

[27] Zhang C, Lu G, Sun Z, Yu J (2012) Catalytic graphitization of carbon/carbon composites by lanthanum oxide. J Rare Earths 30:128–132

[28] Wang R, Lu G, Qiao W, Sun Z, Zhuang H, Yu J (2015) Catalytic effect of praseodymium oxide additive on the microstructure and electrical property of graphite anode. Carbon 95:940–948

[29] Anton R (2008) On the reaction kinetics of Ni with amorphous carbon. Carbon 46:656–662

[30] Murty HN, Biederman DL, Heintz EA (1977) Apparent catalysis of graphitization. 3. Effect of boron, Fuel 56:305–312

[31] Iwashita N, Park CR, Fujimoto H, Shiraishi M, Inagaki M (2004) Specification for a standard procedure of X-ray diffraction measurements on carbon materials. Carbon 42:701–714

[32] Badenhorst H (2014) Microstructure of natural graphite flakes revealed by oxidation: limitations of XRD and Raman techniques for crystallinity estimates. Carbon 66:674–690

[33] Tsukamoto T, Yamazaki K, Komurasaki H, Ogino T (2012) Effects of surface chemistry of substrates on Raman spectra in graphene. J Phys Chem C 116:4732–4737

[34] Torrisi F, Hasan T, Wu W, Sun Z, Lombardo A, Kulmala TS et al (2012) Inkjet-printed graphene electronics. ACS Nano 6:2992–3006

[35] Cançado LG, Takai K, Enoki T, Endo M, Kim YA, Mizusaki H et al (2006) General equation for the determination of the crystallite size La of nanographite by Raman spectroscopy. Appl Phys Lett 88:163106

[36] Franklin RE (1951) Crystallite growth in graphitizing and non-graphitizing carbons. P Roy Soc A-Math Phy 209:196–218

[37] Vázquez-Santos MB, Geissler EK, Rouzaud JN, Martínez-Alonso A, Tascón JMD (2012) Comparative XRD, Raman, and TEM study on graphitization of PBO-derived carbon fibers. J Phys Chem C 116:257–268

[38] Howe JY, Jones LE (2013) Influence of boron on structure and oxidation behavior of graphite fiber, P120. Carbon 42:461–467

[39] Zhai D, Li B, Kang F, Du H, Xu C (2010) Preparation of mesophase-pitch-based activated carbons for electric double layer capacitors with high energy density. Micropor Mesopor Mat 130:224–228

[40] Dresselhaus MS, Jorio A, Saito R (2010) Characterizing graphene, graphite, and carbon nanotubes by Raman spectroscopy. Annu Rev Conden Matt Phys 1:89–108